

Predictions for $\eta_c \rightarrow \eta\pi^+\pi^-$ producing $f_0(500)$, $f_0(980)$ and $a_0(980)$

V. R. Debastiani,^{1,2,*} Wei-Hong Liang,^{3,†} Ju-Jun Xie,^{1,‡} and E. Oset^{1,2,§}

¹*Institute of Modern Physics, Chinese Academy of Sciences, Lanzhou 730000, China*

²*Departamento de Física Teórica and IFIC, Centro Mixto Universidad de Valencia-CSIC
Institutos de Investigación de Paterna, Aptdo. 22085, 46071 Valencia, Spain*

³*Department of Physics, Guangxi Normal University, Guilin 541004, China*

(Dated: September 30, 2016)

We perform calculations for the $\eta_c \rightarrow \eta\pi^+\pi^-$ decay using elements of SU(3) symmetry to see the weight of different trios of pseudoscalars produced in this decay, prior to the final state interaction of the mesons. After that, the interaction of pairs of mesons, leading finally to $\eta\pi^+\pi^-$, is done using the chiral unitary approach. We evaluate the $d\Gamma/dM_{\pi^+\pi^-}$ and $d\Gamma/dM_{\pi^+\eta}$ mass distributions and find large and clean signals for $f_0(500)$, $f_0(980)$ and $a_0(980)$ excitation. The reaction is similar to the $\chi_{c1} \rightarrow \eta\pi^+\pi^-$, which has been recently measured at BESIII and its implementation and comparison with these predictions will be very valuable to shed light on the nature of the low mass scalar mesons.

PACS numbers:

I. INTRODUCTION

The sector of light scalar mesons has been a topic of intense discussions for years [1–5]. Early discussions on their nature as $q\bar{q}$ or more complex objects have converged to accept that these states cannot be $q\bar{q}$ objects. An extensive updated discussion on the issue can be seen in the report [6]. The discussions in Ref. [6] reveal the large amount of empirical information favoring a dynamical picture in which the interaction of pseudoscalar mesons in coupled channels and constraints of unitarity generate scalar mesons, which would qualify as multichannel pseudoscalar-pseudoscalar molecular states. The successful picture incorporating the constraints of unitarity in coupled channels and the dynamics of the chiral Lagrangians [7–9] is known as the chiral unitary approach, and either using the inverse amplitude method [10–12] or the coupled channels Bethe-Salpeter equations [13–16], the success in providing an accurate description in the different reactions where these resonances are produced is remarkable. Detailed reviews of such reactions can be seen in Ref. [17] and more recently in Ref. [18] in relation to B , D , Λ_b and Λ_c decays involving these resonances as dynamically generated. Tetraquark pictures have also been invoked [4, 19], but the standard configurations chosen to account for the masses, run into one or another problem in different reactions. A detailed discussion on this issue can be seen in section IV of Ref. [20].

What ultimately sets the balance in favor of one or another theoretical picture is the power to provide an accurate explanation of multiple reactions, and in this

sense there is nothing more convincing than making predictions for reactions not yet measured and having the predictions realized a posteriori by experiment. This is the aim of the present paper where we make predictions for the decay $\eta_c \rightarrow \eta\pi^+\pi^-$ looking into the invariant mass distributions of $\pi\pi$ and $\pi\eta$. In the distributions we find a very clear and strong signal for the $a_0(980)$, and also weaker but clearly seen signals for $f_0(500)$ and $f_0(980)$ excitations. We are confident on the results up to invariant masses of about 1200 MeV and propose the measurement of the reaction that can easily be implemented in BESIII.

There is a precedent for the $\eta_c \rightarrow \eta\pi^+\pi^-$ reaction in the $\chi_{c1} \rightarrow \eta\pi^+\pi^-$ decay, which has been measured at BESIII (preliminary results are already available [21]). In this reaction one can see a neat $a_0(980)$ signal in the $\pi\eta$ mass distribution with its typical cusp shape and with very little background. On the other hand, in the $\pi^+\pi^-$ mass spectrum one sees a very clear peak for the $f_0(500)$ and a smaller, but visible peak for the $f_0(980)$. The $\pi^+\pi^-$ spectrum also shows a pronounced signal for the $f_2(1270)$ excitation. A theoretical study for this reaction using the chiral unitary approach has been done in Ref. [22] and a good reproduction of the shapes and relative strengths of the invariant mass distributions was obtained up to about 1200 MeV, the present limit of applicability of the chiral unitary approach in the interaction of pseudoscalar mesons.

The $\eta_c \rightarrow \eta\pi^+\pi^-$ has many things in common to the $\chi_{c1} \rightarrow \eta\pi^+\pi^-$, but also differences. The χ_{c1} has quantum numbers $I^G(J^{PC}) = 0^+(1^{++})$, the η_c has $0^+(0^{-+})$. In the $\chi_{c1} \rightarrow \eta\pi^+\pi^-$, if the $\pi^+\pi^-$ is in S-wave to create the $f_0(500)$ and $f_0(980)$, the η must be in P-wave to conserve angular momentum and parity. In the η_c decay the process can proceed in S-wave. Concerning the $f_2(1270)$ excitation, in the $\chi_{c1} \rightarrow \eta\pi^+\pi^-$ reaction, the same process with η in P-wave, and the $\pi^+\pi^-$ in D-wave, can produce the resonance. In the $\eta_c \rightarrow \eta\pi^+\pi^-$ we will need a D-wave for η in the

*Electronic address: vinicius.rodriques@ific.uv.es

†Electronic address: liangwh@gxnu.edu.cn

‡Electronic address: xiejujun@impcas.ac.cn

§Electronic address: oset@ific.uv.es

production vertex, in addition to the internal D-wave of $\pi^+\pi^-$. This mechanism should be suppressed versus the one of $f_0(500)$ or $f_0(980)$ production and then the signals for the scalar mesons would be cleaner than those in the $\chi_{c1} \rightarrow \eta\pi^+\pi^-$ reaction. With this perspective we perform the calculations and make predictions for the reaction. In the absence of the $f_2(1270)$ excitation we also make predictions for the background. Our limitations to the range below 1200 MeV for the energies of the interacting meson pairs, induce uncertainties on the background, but we can show that these uncertainties are small in the region of $\pi^+\pi^-$ or $\pi\eta$ invariant masses below 1200 MeV, thus making our predictions really solid. With these results and clear predictions, we can only encourage the performance of the experiment which is easily implementable at BESIII.

II. FORMALISM

We follow closely the work of [22] with the particular differences of this case. As commented before, the

process proceeds in S-wave. We consider that η_c behaves as a singlet of SU(3), since it does not have u, d, s quarks and, hence, we must construct an SU(3) singlet with the product of three pseudoscalars. For this we write the $q\bar{q}$ matrix

$$M = \begin{pmatrix} u\bar{u} & u\bar{d} & u\bar{s} \\ d\bar{u} & d\bar{d} & d\bar{s} \\ s\bar{u} & s\bar{d} & s\bar{s} \end{pmatrix}, \quad (1)$$

and we find that [22]

$$MMM = M(\bar{u}u + \bar{d}d + \bar{s}s)^2. \quad (2)$$

Since $(\bar{u}u + \bar{d}d + \bar{s}s)$ is already an SU(3) scalar, the scalar that we can construct from MMM is the trace of $M(\bar{u}u + \bar{d}d + \bar{s}s)^2$, and then

$$\text{Trace}[M(\bar{u}u + \bar{d}d + \bar{s}s)^2] = \text{Trace}[MMM]. \quad (3)$$

By writing M in terms of the physical mesons with the matrix ϕ we have

$$M \rightarrow \phi \equiv \begin{pmatrix} \frac{1}{\sqrt{2}}\pi^0 + \frac{1}{\sqrt{3}}\eta + \frac{1}{\sqrt{6}}\eta' & \pi^+ & K^+ \\ \pi^- & -\frac{1}{\sqrt{2}}\pi^0 + \frac{1}{\sqrt{3}}\eta + \frac{1}{\sqrt{6}}\eta' & K^0 \\ K^- & \bar{K}^0 & -\frac{1}{\sqrt{3}}\eta + \sqrt{\frac{2}{3}}\eta' \end{pmatrix}. \quad (4)$$

Then we obtain

$$\begin{aligned} \text{SU}(3)[\text{scalar}] &\equiv \text{Trace}(\phi\phi\phi) = \\ &= \frac{6}{\sqrt{3}}\eta\pi^+\pi^- + \frac{3}{\sqrt{3}}\eta\pi^0\pi^0 + \frac{1}{3\sqrt{3}}\eta\eta\eta \\ &+ 3\pi^+K^0K^- + 3\pi^-K^+\bar{K}^0. \end{aligned} \quad (5)$$

This expression gives us the relative weights in which trios of pseudoscalars are produced from η_c decay in a first step, prior to the final state interaction of these mesons.

The next step is to allow them to interact. By letting all possible pairs to interact and make transitions, and isolating the final $\eta\pi^+\pi^-$ channel, the diagrams to be considered are given in Fig. 1

In the loops of Fig. 1 we show all pairs allowed by Eq. (5) that can give rise to the considered final state. Then the amplitude that sums all terms is given by

$$t = t_{tree} + t_\eta + t_{\pi^+} + t_{\pi^-}, \quad (6)$$

where the tree-level amplitude is

$$t_{tree} = V_p h_{\eta\pi^+\pi^-}, \quad (7)$$

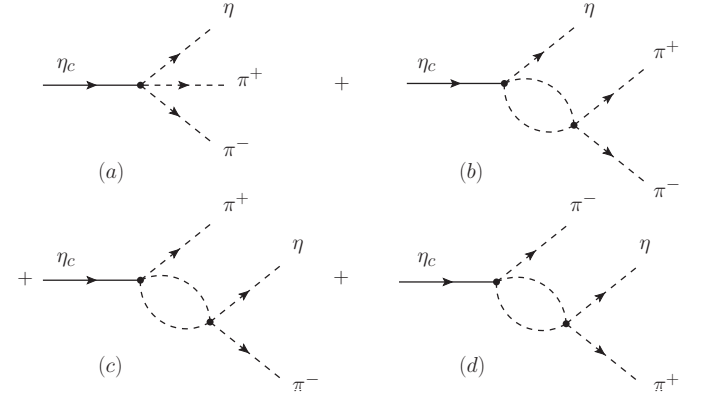


FIG. 1: Diagrams involved in the $\eta_c \rightarrow \eta\pi^+\pi^-$ including final state interaction of pairs.

and the first transition amplitude is

$$t_\eta = V_p \sum_i h_i S_i G_i(M_{\text{inv}}(\pi^+\pi^-)) t_{i,\pi^+\pi^-}(M_{\text{inv}}(\pi^+\pi^-)), \quad (8)$$

where V_p is a constant coefficient, common to all four terms, that accounts for the matrix element of the tree-level $\eta_c \rightarrow 3$ mesons transition, up to h_i coefficients,

which are the factors multiplying each combination of three mesons in Eq. (5). The values of h_i are

$$\begin{aligned} h_{\eta\pi^+\pi^-} &= \frac{6}{\sqrt{3}}, & h_{\eta\pi^0\pi^0} &= \frac{3}{\sqrt{3}}, \\ h_{\eta\eta\eta} &= \frac{1}{3\sqrt{3}}, & h_{\pi^+K^0K^-} &= h_{\pi^-K^+\bar{K}^0} = 3. \end{aligned} \quad (9)$$

In Eq. (8) only $h_{\eta\pi^+\pi^-}$, $h_{\eta\pi^0\pi^0}$ and $h_{\eta\eta\eta}$ contribute. The function G_i is the loop function of the two intermediate mesons and $t_{i,\pi^+\pi^-}$ is the transition matrix element from the state i to $\pi^+\pi^-$. The G_i and $t_{i,\pi^+\pi^-}$ functions, depending on the invariant masses of $\pi^+\pi^-$, $M_{\text{inv}}(\pi^+\pi^-)$, are taken from the chiral unitary approach, and we follow Refs. [13, 23–25]. The factor S_i is a symmetry factor to account for identical particles,

$$S_{\pi^0\pi^0} = 2! \frac{1}{2} \quad (\text{for } \pi^0\pi^0), \quad S_{\eta\eta} = 3! \frac{1}{2} \quad (\text{for } \eta\eta). \quad (10)$$

Similarly, we have

$$t_{\pi^+} = V_p \sum_i h_i S_i G_i(M_{\text{inv}}(\pi^-\eta)) t_{i,\pi^-\eta}(M_{\text{inv}}(\pi^-\eta)), \quad (11)$$

where in the sum over i we have the states $\pi^-\eta$ and K^0K^- , and

$$t_{\pi^-} = V_p \sum_i h_i S_i G_i(M_{\text{inv}}(\pi^+\eta)) t_{i,\pi^+\eta}(M_{\text{inv}}(\pi^+\eta)), \quad (12)$$

where now in i we have $\pi^+\eta$ and $K^+\bar{K}^0$.

We take as reference the $\pi^+\pi^-$ and $\pi^+\eta$ invariant masses and write the double differential distribution [26]

$$\begin{aligned} & \frac{d^2\Gamma}{dM_{\text{inv}}(\pi^+\pi^-)dM_{\text{inv}}(\pi^+\eta)} \\ &= \frac{1}{(2\pi)^3} \frac{1}{8M_{\eta c}^3} M_{\text{inv}}(\pi^+\pi^-) M_{\text{inv}}(\pi^+\eta) |t|^2. \end{aligned} \quad (13)$$

From this formula we obtain $\frac{d\Gamma}{dM_{\text{inv}}(\pi^+\pi^-)}$ and $\frac{d\Gamma}{dM_{\text{inv}}(\pi^+\eta)}$ by integrating over the other invariant mass. By labeling 1, 2, 3 to the η , π^+ , π^- particles, respectively, if we integrate over M_{23} , the limits of integration are given in Ref. [26] by

$$\begin{aligned} (M_{23}^2)_{\text{max}} &= (E_2^* + E_3^*)^2 \\ &\quad - (\sqrt{E_2^{*2} - m_2^2} - \sqrt{E_3^{*2} - m_3^2})^2, \\ (M_{23}^2)_{\text{min}} &= (E_2^* + E_3^*)^2 \\ &\quad - (\sqrt{E_2^{*2} - m_2^2} + \sqrt{E_3^{*2} - m_3^2})^2, \end{aligned} \quad (14)$$

where

$$\begin{aligned} E_2^* &= (M_{12}^2 - m_1^2 + m_2^2)/2M_{12}, \\ E_3^* &= (M_{12}^2 - M_{12}^2 + m_3^2)/2M_{12}. \end{aligned} \quad (15)$$

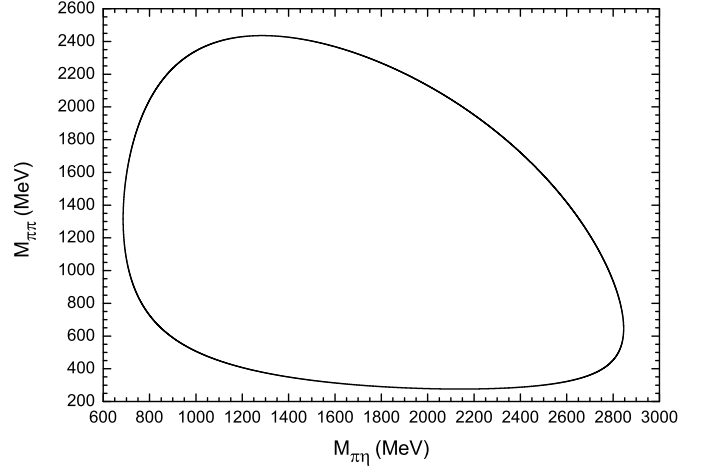


FIG. 2: Dalitz Plot for $\eta_c \rightarrow \eta\pi^+\pi^-$, in the $\pi\eta$ and $\pi\pi$ masses.

If we integrate over M_{12} , the limits of integration are

$$\begin{aligned} (M_{12}^2)_{\text{max}} &= (E_2^{*'} + E_1^{*'})^2 \\ &\quad - (\sqrt{E_2^{*'}^2 - m_2^2} - \sqrt{E_1^{*'}^2 - m_1^2})^2, \\ (M_{12}^2)_{\text{min}} &= (E_2^{*'} + E_1^{*'})^2 \\ &\quad - (\sqrt{E_2^{*'}^2 - m_2^2} + \sqrt{E_1^{*'}^2 - m_1^2})^2, \end{aligned} \quad (16)$$

where

$$\begin{aligned} E_2^{*'} &= (M_{23}^2 - m_3^2 + m_2^2)/2M_{23}, \\ E_1^{*'} &= (M_{\eta c}^2 - M_{23}^2 + m_1^2)/2M_{23}. \end{aligned} \quad (17)$$

Since we take the $\pi^+\pi^-$ and $\pi^+\eta$ invariant masses as variables, we must note that t_{π^-} depends on the $\pi^-\eta$ invariant mass, M_{13} . However, this mass is given in terms of the other two variables since one has

$$M_{13}^2 = M_{\eta c}^2 + m_\pi^2 + m_\pi^2 + m_\eta^2 - M_{12}^2 - M_{23}^2. \quad (18)$$

III. RESULTS

In Fig. 2 we show the Dalitz plot for $M_{\pi\pi}$ and $M_{\pi\eta}$ in the $\eta_c \rightarrow \eta\pi^+\pi^-$ decay. We are interested in $\frac{d\Gamma}{dM_{\text{inv}}(\pi^+\pi^-)}$ and $\frac{d\Gamma}{dM_{\text{inv}}(\pi^+\eta)}$ in the region of $f_0(500)$, $f_0(980)$ and $a_0(980)$. If we take $M_{\pi\eta} \sim 1000$ MeV we see that $M_{\pi\pi}$ goes from 500-2300 MeV, but the range is similar for values of $M_{\pi\eta}$ up to 2400 MeV. This means that the strength of the $\pi\pi$ distribution will be spread along a wide range of $M_{\pi\eta}$ and we expect roughly a background following phase space. At $M_{\pi\eta} \sim 750$ MeV the range of $M_{\pi\pi}$ is reduced to 800-1700 MeV and we can expect to obtain contribution from the $M_{\pi\pi} \sim 980$ MeV region, which we have under control. Altogether we might anticipate that the background below the $a_0(980)$ peak will be moderate and controllable.

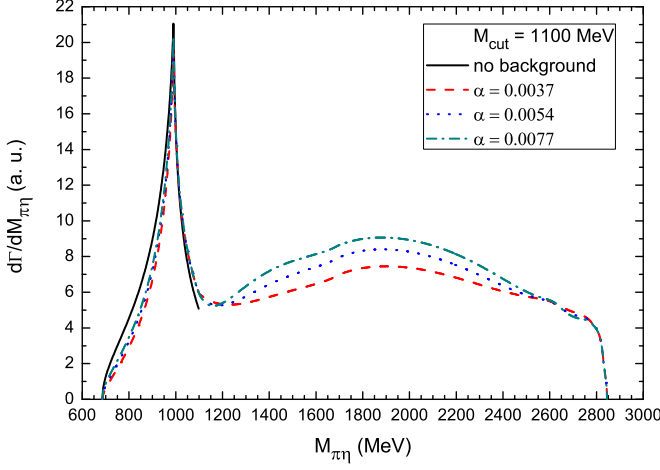


FIG. 3: (Color online) $\frac{d\Gamma}{dM_{\pi\eta}}$ as a function of $M_{\pi\eta}$ for $M_{\text{cut}} = 1100$ MeV and three different values of α . See text for explanations.

If we now fix $M_{\pi\pi}$ in 500-1000 MeV, the range of $M_{\pi\eta}$ is large and we should expect a background evenly distributed according to phase space. However, for $M_{\pi\pi} \sim 400$ MeV the range of $M_{\pi\eta}$ begins at 1200 MeV, thus for these energies we will not have contribution from the large peak of the $a_0(980)$ and the background will be small.

In order to evaluate the differential mass distributions we must bear in mind that the chiral unitary approach that we use only makes reliable predictions up to 1100-1200 MeV. One should not use the model for higher invariant masses. With this perspective we will have to admit uncertainties in the mass distributions, particularly at invariant masses higher than 1200 MeV which are a large part of the Dalitz plot. Yet, we are only interested in the region of invariant masses below 1200 MeV both in $M_{\pi\pi}$ and $M_{\pi\eta}$ and it is just there where we would like to know uncertainties of our model. For that purpose we take the following prescription: we evaluate $Gt(M_{\text{inv}})$ combinations up to $M_{\text{inv}} = M_{\text{cut}}$. From there on we multiply Gt by a smooth factor to make it gradually decrease at large M_{inv} . Thus we take

$$Gt(M_{\text{inv}}) = Gt(M_{\text{cut}})e^{-\alpha(M_{\text{inv}} - M_{\text{cut}})}, \quad \text{for } M_{\text{inv}} > M_{\text{cut}}. \quad (19)$$

We take the values $M_{\text{cut}} = 1100$ MeV and 1150 MeV, with $\alpha = 0.0037 \text{ MeV}^{-1}$, 0.0054 MeV^{-1} and 0.0077 MeV^{-1} , which reduce Gt by about a factor 3, 5 and 10, respectively at $M_{\text{cut}} + 300$ MeV. We show the results in Figs. 3, 4, 5 for $\frac{d\Gamma}{dM_{\text{inv}}(\pi^+\pi^-)}$ and Figs. 6, 7, 8 for $\frac{d\Gamma}{dM_{\text{inv}}(\pi^+\pi^-)}$.

In Fig. 3 we show our results for $\frac{d\Gamma}{dM_{\text{inv}}(\pi^+\pi^-)}$ (the $\frac{d\Gamma}{dM_{\text{inv}}(\pi^+\pi^-)}$ is identical). The results are obtained with $M_{\text{cut}} = 1100$ MeV and the three values of α . What we see is that from 1200 MeV on we have appreciable uncertainties, but below this energy, in the region of

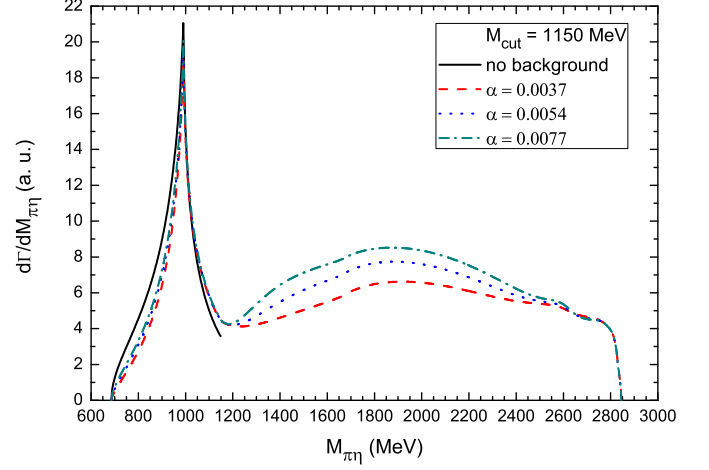


FIG. 4: (Color online) Same as Fig. 3 for $M_{\text{cut}} = 1150$ MeV.

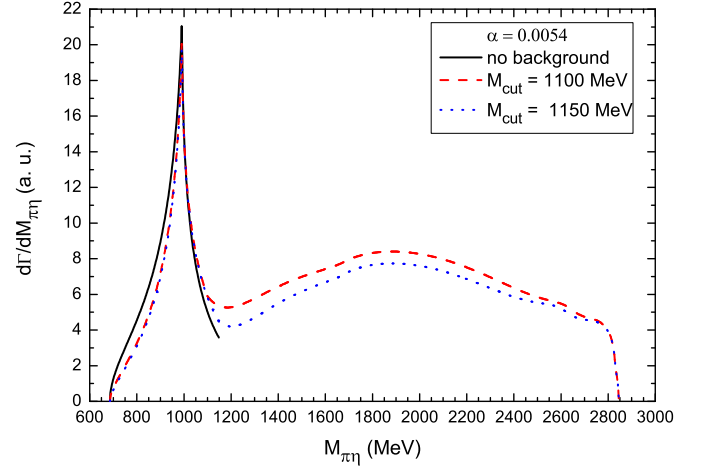


FIG. 5: (Color online) Same as Fig. 3 for two different values of M_{cut} and one value of α .

the $a_0(980)$ the uncertainties are very small, what makes the predictions in that region rather reliable. Since the amplitude t of Eq. (6) sums coherently all terms, it is interesting to see what is mostly responsible for the peak. For this we keep in t the tree-level amplitude t_{tree} and t_{π^-} , since t_{π^-} is the term that contains the direct $M_{\text{inv}}(\pi^+\eta)$ dependence in $t_{i,\pi^+\eta}(M_{\text{inv}}(\pi^+\eta))$. The result obtained with only these two terms are shown in Fig. 3 by the solid line. This is what we call in the figure, “no background”. We can see that the “background” created in that region by the other two terms, t_{π^+} and t_η is rather small. Yet, in the region from $M_{\pi\eta} = 700$ MeV to 990 MeV, this “background” reduces a bit the contribution obtained by $t_{\text{tree}} + t_{\pi^-}$ only. It is interesting to note that the “no background” prescription was taken in [22] and a smooth background was added incoherently to the $\pi\pi$ mass distributions in the $\chi_{c1} \rightarrow \eta\pi^+\pi^-$, but not to the $\pi\eta$ mass distribution. The $a_0(980)$ mass distribution was in quite good agreement with experiment [21], but

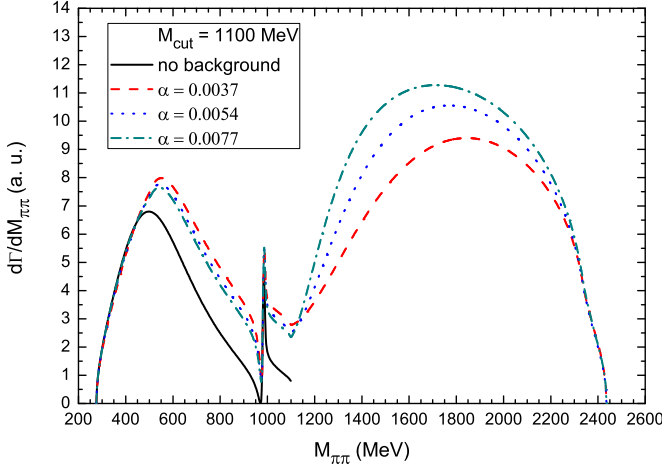


FIG. 6: (Color online) $\frac{d\Gamma}{dM_{\pi\pi}}$ as a function of $M_{\pi\pi}$ for $M_{\text{cut}} = 1100$ MeV and three different values of α . See text for explanations.

was a bit higher in the $M_{\pi\eta} = 700 - 990$ MeV region, by an amount similar to the difference seen in Fig. 3 between the solid and other curves. The results obtained here could be easily translated there, with the consequent improvement of the agreement with the data. Similarly, at energies above 1050 MeV the “background” increases the “no background” curve, and this would also help the results of [22] to get in better agreement with the data of [21].

The strong cusp shape of the $a_0(980)$ and the small background, qualify this reaction, together with the $\chi_{c1} \rightarrow \eta\pi^+\pi^-$, as the reaction where $a_0(980)$ shows up more strongly and more neatly.

In Fig. 4, we show the same results but now $M_{\text{cut}} = 1150$ MeV. The results are similar and the uncertainties in the region of $M_{\pi\eta} > 1200$ MeV are a bit bigger than before. What matters for our purpose is that below the $a_0(980)$ region, again the background is small and so are the uncertainties.

In Fig. 5 we present the results with the two M_{cut} values and $\alpha = 0.0054$ MeV $^{-1}$. We can see better here that the results below 1100 MeV are basically the same and not affected by the value chosen for M_{cut} .

In Fig. 6 we show the analogous results of Fig. 3 but for the $\frac{d\Gamma}{dM_{\text{inv}}(\pi^+\pi^-)}$ mass distribution. We see that taking $M_{\text{cut}} = 1100$ MeV, there are uncertainties in the region of $M_{\pi\pi} > 1200$ MeV for the different values of α chosen, but the uncertainties are much smaller in the region below 1200 MeV, what makes the predictions done more solid. It is more interesting to see that we observe a neat signal for the $f_0(500)$ and a much smaller, but clearly visible, signal for the $f_0(980)$. We also show the results with “no background” obtained taking for t the sum $t_{\text{tree}} + t_\eta$, since in t_η we have the terms $t_{i,\pi^+\pi^-}(M_{\text{inv}}(\pi^+\pi^-))$. We can see that the “background” does not affect the mass distribution below 450 MeV, but gives a sizeable contribution from 550 MeV to 1200 MeV. Once more,

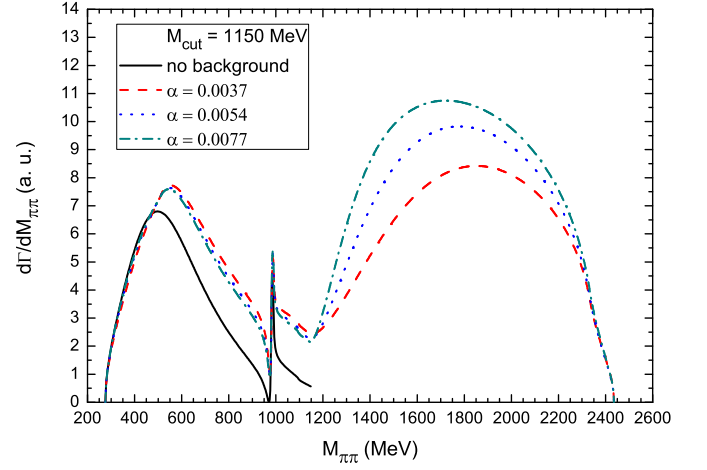


FIG. 7: (Color online) Same as Fig. 6 for $M_{\text{cut}} = 1150$ MeV.

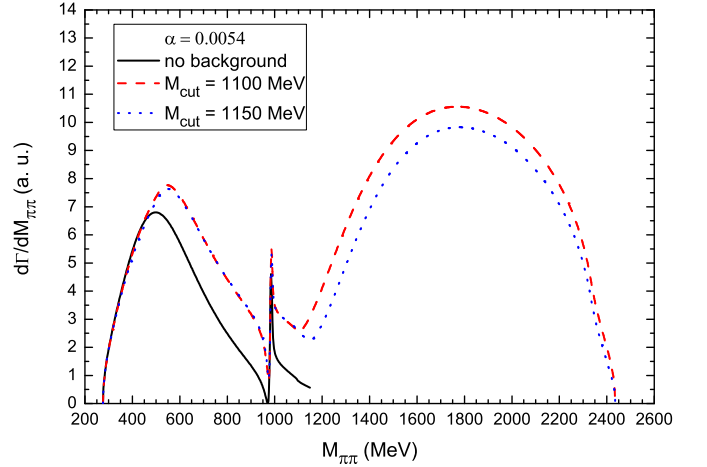


FIG. 8: (Color online) Same as Fig. 6 for two different values of M_{cut} and one value of α .

in the $\chi_{c1} \rightarrow \eta\pi^+\pi^-$ reaction studied in [22], where only the “no background” terms were considered, it was found that an “empirical” background of this size was needed to reproduce the data of [21]. Again, all these facts reinforce the reliability of the predictions made here.

In Fig. 7 we show the results for $M_{\text{cut}} = 1150$ MeV. They are similar to those of Fig. 6, with the uncertainties in the region of $M_{\pi\pi} > 1200$ MeV a bit bigger. However, below the $M_{\pi\pi} = 1200$ MeV the results are practically identical. This is better seen in Fig. 8, where we show the results for the two values of M_{cut} and $\alpha = 0.0054$ MeV $^{-1}$. We see indeed, that the region below 1200 MeV is not affected by the choice of M_{cut} .

The results obtained are shown in arbitrary units (the calculations are done taking a value of $V_p = 100$), however, the relative weights for the $M_{\pi\pi}$ and $M_{\pi\eta}$ mass distributions of the figures are also predictions that can be tested in actual experiment. As we can see, the strength of the peak of the $a_0(980)$ is about three times

the strength of the $f_0(500)$ peak.

We should note that in the region of $M_{\pi\pi}$ or $M_{\pi\eta}$ above 1200 MeV one should expect contribution from other resonances, not accounted for here. However, the small uncertainties of the spectrum below 1200 MeV due to the uncertainties above 1200 MeV, indicate that the corrections below 1200 MeV due to the contribution of higher energy resonances would still be small.

IV. CONCLUSIONS

We have done a theoretical study of the $\eta_c \rightarrow \eta\pi^+\pi^-$ decay paying attention to the final state interaction of the pairs of mesons. We evaluate $\frac{d\Gamma}{dM_{\text{inv}}(\pi^+\pi^-)}$ and $\frac{d\Gamma}{dM_{\text{inv}}(\pi^+\eta)}$ and make predictions that should be confronted by a future experiment. The first step is to see the weight of the possible trios of mesons coming from η_c decay, prior to any final state interaction, which is done assuming that η_c is an SU(3) singlet and then using SU(3) symmetry in the trios of pseudoscalar mesons. After that, the interaction of all possible pairs in the trios (not only $\eta\pi^+\pi^-$) are allowed to interact, leading to the final $\eta\pi^+\pi^-$. The calculations are done using the chiral unitary approach for the interaction of mesons, which has a limit of applicability up to $M_{\text{inv}} = 1200$ MeV. We observe a large and clean signal for the $a_0(980)$ in the $\pi^+\eta$ mass distribution, and a relatively large signal for $f_0(500)$ and a smaller one for $f_0(980)$ in the $\pi^+\pi^-$ mass distribution.

Given our ignorance above 1200 MeV, we kill gradually the loop functions and amplitudes beyond a M_{cut} around 1200 MeV and, with different options, we estimate uncertainties. What we observe in that, while uncertainties indeed appear in the region of $M_{\text{inv}} > 1200$ MeV, they are very small below that energy, rendering our predictions rather solid. The shape and strength of the mass distributions, up to a global factor, the same for all of them, are predictions of the theory which could be confronted with experiment. The ultimate aim would be to provide support to the picture in which the $f_0(500)$, $f_0(980)$ and $a_0(980)$ resonances are dynamically generated from the pseudoscalar-pseudoscalar interaction. Since neat predictions, more than reproduction of measured data, have a higher value to support one or another picture for the scalar mesons, we encourage both, calculations of the reaction in different models, as well as the performance of the reaction, which in analogy to the $\chi_{c1} \rightarrow \eta\pi^+\pi^-$ already measured at BESIII, could be measured in this or other facilities.

Acknowledgments

One of us, V. R. D. wishes to acknowledge the support from the Programa Santiago Grisolia of Generalitat Valenciana. One of us, E. O. wishes to acknowledge the

support from the Chinese Academy of Science in the Program of Visiting Professorship for Senior International Scientists (Grant No. 2013T2J0012). This work is partly supported by the National Natural Science Foundation of China under Grants No. 11565007, No. 11547307 and No. 11475227. It is also supported by the Youth Innovation Promotion Association CAS (No. 2016367). This work is also partly supported by the Spanish Ministerio de Economia y Competitividad and European FEDER funds under the contract number FIS2011-28853-C02-01, FIS2011-28853-C02-02, FIS2014-57026-REDT, FIS2014-51948-C2-1-P, and FIS2014-51948-C2-2-P, and the Generalitat Valenciana in the program Prometeo II-2014/068.

-
- [1] E. Klempt and A. Zaitsev, Phys. Rept. **454**, 1 (2007)
 - [2] E. van Beveren, T. A. Rijken, K. Metzger, C. Dullemond, G. Rupp and J. E. Ribeiro, Z. Phys. C **30**, 615 (1986)
 - [3] N. A. Tornqvist and M. Roos, Phys. Rev. Lett. **76**, 1575 (1996)
 - [4] A. H. Fariborz, R. Jora and J. Schechter, Phys. Rev. D **79**, 074014 (2009)
 - [5] A. H. Fariborz, N. W. Park, J. Schechter and M. Naeem Shahid, Phys. Rev. D **80**, 113001 (2009)
 - [6] J. R. Pelaez, arXiv:1510.00653 [hep-ph], to be published in Phys. Reports.
 - [7] S. Weinberg, Physica A **96**, 327 (1979).
 - [8] J. Gasser and H. Leutwyler, Annals Phys. **158**, 142 (1984).
 - [9] V. Bernard, N. Kaiser and U. G. Meissner, Int. J. Mod. Phys. E **4**, 193 (1995)
 - [10] A. Dobado and J. R. Pelaez, Phys. Rev. D **56**, 3057 (1997)
 - [11] J. R. Pelaez and G. Rios, Phys. Rev. Lett. **97**, 242002 (2006)
 - [12] J. A. Oller, E. Oset and J. R. Pelaez, Phys. Rev. D **59**, 074001 (1999) Erratum: [Phys. Rev. D **60**, 099906 (1999)] Erratum: [Phys. Rev. D **75**, 099903 (2007)]
 - [13] J. A. Oller and E. Oset, Nucl. Phys. A **620**, 438 (1997) Erratum: [Nucl. Phys. A **652**, 407 (1999)]
 - [14] N. Kaiser, Eur. Phys. J. A **3**, 307 (1998).
 - [15] M. P. Locher, V. E. Markushin and H. Q. Zheng, Eur. Phys. J. C **4**, 317 (1998)
 - [16] J. Nieves and E. Ruiz Arriola, Nucl. Phys. A **679**, 57 (2000)
 - [17] J. A. Oller, E. Oset and A. Ramos, Prog. Part. Nucl. Phys. **45**, 157 (2000)
 - [18] E. Oset *et al.*, Int. J. Mod. Phys. E **25**, 1630001 (2016)
 - [19] R. L. Jaffe, Phys. Rev. D **15**, 267 (1977), Phys. Rev. D **15**, 281 (1977).
 - [20] J. M. Dias, F. S. Navarra, M. Nielsen and E. Oset, arXiv:1601.04635 [hep-ph].
 - [21] M. Kornicer [BESIII Collaboration], AIP Conf. Proc. **1735**, 050011 (2016).
 - [22] W. H. Liang, J. J. Xie and E. Oset, arXiv:1609.03864 [hep-ph].
 - [23] W. H. Liang and E. Oset, Phys. Lett. B **737**, 70 (2014)
 - [24] J. J. Xie, L. R. Dai and E. Oset, Phys. Lett. B **742**, 363 (2015)
 - [25] W. H. Liang, J. J. Xie and E. Oset, Phys. Rev. D **92**, no. 3, 034008 (2015)
 - [26] K. A. Olive *et al.* [Particle Data Group Collaboration], Chin. Phys. C **38**, 090001 (2014).